Laser Produced Hemispherical Shock Waves

BARRETT S. ROBB* AND DONALD L. TURCOTTE†
Cornell University, Ithaca, N.Y.

An experimental study of laser induced hemispherical shock waves has been carried out. A Q-switched ruby laser was focused on aluminum or carbon targets and the plasma produced expanded into an ambient atmosphere of argon or helium. Trajectories of the primary and secondary shock waves were determined for initial pressures from 0.05 to 5 torr. Spherical blast wave theory was found to apply for radii greater than the mass length, $(M/\rho_0)^{1/3}$, where M is the plasma mass and ρ_0 the background gas density. The results are compared with previous numerical solutions, and several rules for secondary shock wave behavior are stated.

Nomenclature

a = sound velocity
c_v = specific heat at constant volume
E = energy of explosion
k = Boltzmann's constant
L_E = energy length
L_M = mass length
m = molecular weight
M = driver gas mass
p = pressure
R = shock wave radius
t = time
T = temperature
V = gas velocity
y = log-log trajectory slope
α = nondimensional constant
γ = ratio of specific heats
ε = specific energy
λ = nondimensional radius
ρ = density

Subscripts
0 = ambient atmosphere
1 = driver gas
2 = secondary shock
max = maximum radius
ret = return to origin

Introduction

SOLID-STATE lasers, especially high power Q-switched lasers, have been used as energy sources in plasma experiments. When focused on a small area, Q-switched lasers can generate 10^9 to 10^{12} w/cm^2. This is far above the power densities necessary to vaporize and ionize solid material on time scales of nanoseconds. The emitted ions provide a good source of high temperature plasmas for experiments. Many authors have focused lasers on thick, solid targets in a vacuum.[1-4] Measurements of maximum electron temperature in the plasma range from 10 ev[5] to about 35 ev.[6]

If the laser-produced plasma is allowed to expand into an ambient atmosphere instead of into a vacuum, the plasma acts as an explosive and drives a strong, nearly-hemispherical shock wave ahead of it. Experimental studies of laser-produced explosions have been carried out by Basov et al.,[7] Bobin et al.,[8] and Hall.[9] These studies indicated that the primary shock wave obeyed blast wave theory[10,11] after the energy addition by the laser pulse ended. Secondary shock waves were not reported in laser produced explosions.

In the present experiment[12] the trajectory of the primary shock wave has been studied and compared with blast wave theory. In addition, secondary shock waves within the driver gas have been photographed. The results of this study show disagreement with the previous experimental investigations, but confirm and extend the conclusions of previous numerical calculations of explosion problems.

Theory

Similarity solutions for spherical-explosion problems have been obtained by Taylor[10] and Sedov[11] for a point-source addition of energy. The primary shock trajectory was found to be

$$R = (\alpha E/\rho_0)^{1/5} t^{2/5} \tag{1}$$

The above relation assumes that the shock wave is strong and that no mass has been added.

A similarity solution is not possible for explosions in which a finite amount of mass is added to the flow. However, numerical solutions[13-16] have been carried out to determine the flowfield in this case. The typical problem studied in these investigations is a spherical shock-tube explosion, i.e., a sphere of static, high-pressure gas released into an ambient atmosphere. The calculations show that the primary shock wave does not follow blast-wave theory until it has engulfed a mass of atmosphere much greater than the mass of the driver gas. In addition, a secondary shock wave forms which propagates into the driver gas from the contact surface.

The presence of the secondary shock wave can be explained as follows. Near the beginning of the explosion the primary shock wave transmits a high-pressure back to the contact surface. The driver gas, however, expands spherically and its pressure drops rapidly. From a simplified viewpoint, the driver gas pressure decreases as R^3, while the shock wave strength decreases as R^2.[17] In order to maintain continuity of pressure across the contact surface, the secondary shock wave forms and propagates toward the origin with respect to the driver gas. Because of the high outward expansion velocity, the secondary shock wave is swept outward away from the origin until it is strong enough to overcome the expansion velocity and converge on the origin. Thus, in the laboratory frame of reference, it appears to move outward to a maximum radius and then return to the origin.

We introduce two characteristic lengths which define the range of validity of blast-wave theory. The first, which we call an energy length, is defined as

$$L_E = (E/P_0)^{1/3} \tag{2}$$

Received June 6, 1972; presented as Paper 72-720 at the AIAA 5th Fluid and Plasma Dynamics Conference, Boston, Mass., June 26–28, 1972; revision received December 26, 1972. This research has been supported by the U.S. Air Force Office of Scientific Research under contract F44620-69-C-0063.

Index categories: Shock Waves and Detonations; Lasers.

* Graduate Research Assistant; presently at Bell Telephone Laboratories, Holmdel, N.J. Member AIAA.

† Professor, Sibley School of Mechanical and Aerospace Engineering. Associate Fellow AIAA.

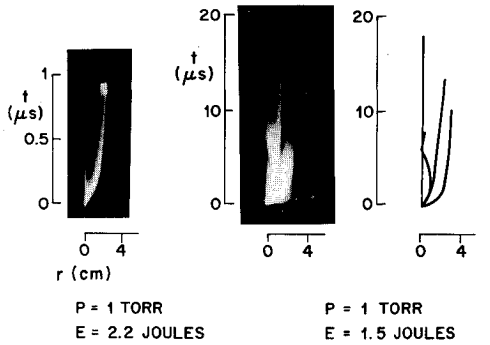

Fig. 1 Typical streak photographs showing primary and secondary shock waves for carbon target in argon.

This length is proportional to the radius at which the energy of the atmosphere engulfed by the shock is equal to the energy of the explosion. Blast-wave theory applies for shock radii much less than L_E.[11] As R approaches L_E, the pressure behind the shock wave becomes comparable to the background pressure, strong shock theory is no longer valid, and no similarity solution exists.

The second characteristic length, called the mass length, is given by

$$L_M = (M/\rho_0)^{1/3} \tag{3}$$

This length is proportional to the radius at which the mass of atmosphere engulfed by the shock is equal to the driver gas mass. Since the similarity solution assumes that $M = 0$, we would expect blast wave theory to be valid for shock radii much greater than L_M. We conclude that blast wave theory is valid in the range

$$L_M \ll R \ll L_E \tag{4}$$

In the experiments reported in this paper L_M varied from 0.5 cm to 4 cm and L_E from 12 cm to 50 cm.

Equipment and Procedure

Hemispherical shock waves have been produced by focusing a Q-switched ruby laser onto the surface of thick, solid targets of carbon and aluminum. Pulse half-widths were about 20 nsec and the energy varied from one to three joules. For the shock wave studies the pressure of the ambient atmosphere of either argon or helium was varied from 0.05 to 5 torr. The primary diagnostic tool was a TRW image-converter camera operated in either the streak or framing mode.

Figure 1 shows two streak photographs of carbon explosions in argon and a diagram showing the shock waves involved. The camera was situated so as to take a side view of the explosions. The laser pulse occurs at $t = 0$, and enters the chamber from the right side as seen in the photographs. Thus the photographs show the extreme outer radius of the shock waves as a function of time. In the 20 μsec duration photograph the primary shock wave is seen to propagate into the ambient atmosphere with a large initial velocity, while the secondary shock wave moves outward to a maximum radius and then returns to the origin. Also visible is the contact discontinuity between the driver gas and the shocked background gas. The 1 μsec streak photograph shows the small time behavior of the primary shock wave. In addition, a secondary shock wave can be seen to slow down and separate from the main shock luminosity.

The mass of the driver plasma as a function of laser energy was deduced by crater volume measurements and by measuring the pressure rise in the chamber immediately after the explosion. Both methods showed a linear relation between laser-pulse energy and plasma mass. Since some of the material ejected from the target is in the form of microparticles which do not participate in the gasdynamic explosion, a crater volume measurement gives an upper limit on the mass addition. It is certainly not clear that a pressure rise measurement will give information on the number of metallic atoms injected since these atoms would tend to adhere to the chamber walls. However, it was found that the pressure measurement was reproducible and was independent of the amount of outgassing of either the chamber or the target. The mass given by the pressure rise measurement was between 5 and 10% of the volume measurement and was in good agreement with the results of David and Weichel.[5] In the results which follow the pressure rise results are used with $M/E = 1.87 \times 10^{-6}$ g/joule for carbon and 4.4 10^{-6} g/joule for aluminum. Since both the pressure rise and crater volume measurements showed a linear dependence of mass on laser energy, only a constant factor is involved. As is shown, the energy per unit mass was constant for each target material over the range of energies used.

Table 1 Average slope of main shock log-log trajectory for $R < L_M$

Pressure, torr	0.5	1	5
Carbon in argon	0.67	0.73	0.65
Carbon in helium	0.58	0.53	0.68
Aluminum in argon	0.62	0.62	0.49
Aluminum in helium		0.50	0.62

Results

Framing photographs showed that the primary shock wave was nearly hemispherical in the cases studied. Primary shock trajectories were obtained from the streak photos and were plotted on log-log paper as R vs t. For the ranges of radius $R < L_M$ and $R > L_M$ the average slope was measured for each set of conditions. Typical log-log plots are shown in Fig. 2. The solid lines on the plots indicate a slope of 2/5. The average slopes of the trajectories for $R < L_M$ are given in Table 1. These are the values of the power y when the shock trajectory is expressed as

$$R \sim t^y \tag{5}$$

For radii greater than L_M the slopes of the trajectories are given in Table 2. The estimated experimental accuracy of the slopes is $\pm 5\%$.

Table 2 Average slope of main shock log-log trajectory for $R > L_M$

Pressure, torr	0.5	1	5
Carbon in argon	0.41	0.40	0.173
Carbon in helium	0.39	0.35	0.32
Aluminum in argon	0.38	0.36	0.254
Aluminum in helium	0.42	0.38	0.38

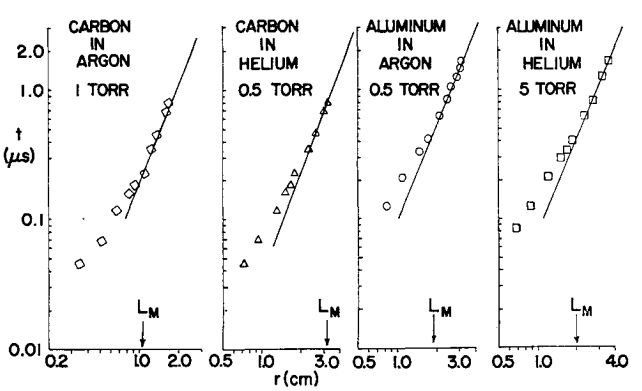

Fig. 2 Typical primary shock wave trajectories.

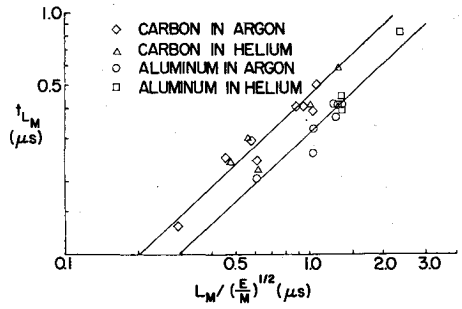

Fig. 3 Dependence of the time at which $R = L_M$ on the characteristic time $L_M/(E/M)^{1/2}$.

It is of interest to note that the values of y for $R < L_M$ are close to the limiting value of 0.69 predicted by Whitham[17] for a spherical shock wave segment traveling through a duct with area proportional to distance squared ($\gamma = 5/3$). Whitham's critical assumption was that the shock wave motion was unaffected by the piston motion behind it. It appears that in the present experiment, the small time motion of the main shock meets this requirement to some extent. Friedman[18] also used this result in an approximate solution of the spherical explosion problem. Of course the intricate wave pattern set up between the contact surface and the shock causes the shock to conform to blast wave theory. As we shall see, this occurs near $R = L_M$.

At pressures of 0.5 and 1 torr the exponents for $R > L_M$ were quite close to the blast wave value of 2/5. However, at 5 torr the exponents were much smaller. This was due to the low Mach number of the shock at this high pressure. The photographs show the self-luminosity due to excitation behind the shock wave. When the Mach number fell below about 10, the luminosity became too low to be observed. The luminous front measured at these Mach numbers was probably due to the atoms previously excited by the shock wave, and therefore underestimates the shock radius.

We wish to find a small time equivalence principle, i.e., a transformation which makes the early trajectories of the primary shock coincide for varying initial conditions. We know from the R vs t plots that in every explosion the transition to blast wave behavior occurred near $R = L_M$. If we plot the trajectories as R/L_M vs t, the transition points would all occur near $R/L_M = 1$. We wish to find a characteristic time which determines the time of transition to blast wave behavior. A characteristic velocity can be found by equating the kinetic energy of the shocked atmosphere when the shock is at $R = L_M$, to the original energy of the explosion

$$E = \tfrac{1}{2}\rho_0(\tfrac{2}{3}\pi L_M{}^3)V^2 \tag{6}$$

And using Eq. (3), we find

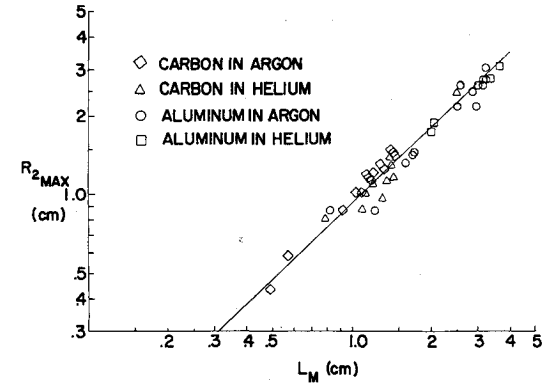

Fig. 5 Dependence of the maximum radius of the secondary shock wave on the mass length.

$$V \sim (E/M)^{1/2} \tag{7}$$

This velocity is related to the driver gas sound speed since

$$a_1 = (\gamma kT/m)^{1/2} \sim (E/M)^{1/2} \tag{8}$$

We would expect the driver sound speed to appear, because for an infinite pressure ratio the initial shock velocity is $a_1(\gamma_0+1)/(\gamma_1-1)$. Using $(E/M)^{1/2}$ as a characteristic velocity with the mass length, L_M, a characteristic time $L_M/(E/M)^{1/2}$ is defined. For the present experiments $(E/M)^{1/2} = 2.32 \times 10^6$ cm/sec for carbon and $(E/M)^{1/2} = 1.51 \times 10^6$ cm/sec for aluminum.

We define t_{L_M} as the time of arrival of the primary shock wave at $R = L_M$. A plot of t_{L_M} as a function of $L_M/(E/M)^{1/2}$ is given in Fig. 3. As can be seen, for each target material $t_{L_M}/L_M(M/E)^{1/2}$ was nearly constant, and was independent of background gas. Standard deviations from the mean were about 15%, which can be considered fairly good agreement for this type of experiment. For each target material then, an early time equivalence existed such that the primary shock wave attained a radius, $R = L_M$ at a time determined by the characteristic time, $L_M/(E/M)^{1/2}$.

Next we consider the motion of the secondary shock wave. For each explosion we know E, M, p_0, ρ_0, as well as L_E and L_M. The most obvious measurement is the maximum radius of the secondary shock wave, $R_{2_{max}}$. This can be measured directly from the streak photos. Since L_E is the commonly used length scale in explosion problems, we first plot $R_{2_{max}}$ against L_E. In Fig. 4 we can see by inspection that each combination of target material and background gas shows a direct dependence of $R_{2_{max}}$ on L_E. This suggests that the atomic weight of the gas may be an important factor since L_E does not account for background density variations which are independent of pressure.

Therefore, a plot of $R_{2_{max}}$ vs L_M was made as shown in Fig. 5.

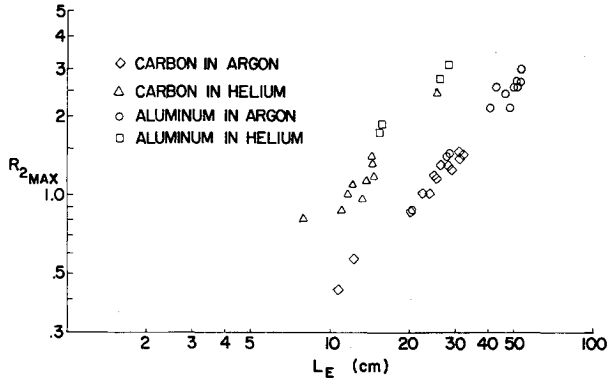

Fig. 4 Dependence of the maximum radius of the secondary shock wave on the energy length.

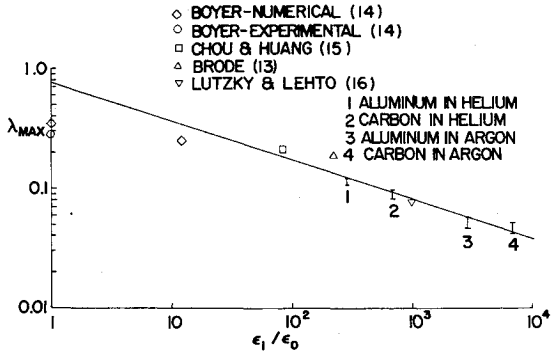

Fig. 6 Dependence of $\lambda_{max} = R_{2_{max}}/L_E$ on the initial specific energy ratio.

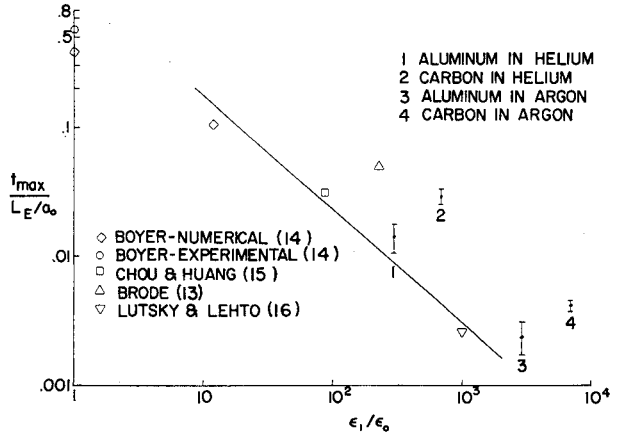

Fig. 7 Dependence of the nondimensional time at which the secondary shock wave is at its maximum radius on the initial specific energy ratio.

Within reasonable limits this is a straight line of slope unity. The standard deviation from the mean of $R_{2_{max}}/L_M$ was about 8%. Thus the measurements show that the maximum radius of the secondary shock wave was linearly proportional to the mass length of the explosion.

Lutzky and Lehto[16] found by numerical calculations that for a large initial density ratio, ρ_1/ρ_0 in the spherical shock tube explosion, the path of the secondary shock wave depended only on the initial ratio of specific internal energies. The shock trajectory was plotted as R_2/L_E vs ta_0/L_E. In the present experiment we define the specific internal energy of the driver gas as the laser energy divided by the vaporized mass. Since these were linearly proportional, the specific energy $\varepsilon_1 = E/M$, using the notation of Lutzky and Lehto, was a constant for each target material; $\varepsilon_1 = 5.34 \times 10^{12}$ ergs/g for carbon and $\varepsilon_1 = 2.27 \times 10^{12}$ ergs/g for aluminum. The specific internal energy of the background gas is given by

$$\varepsilon_0 = c_V T_0 \tag{9}$$

For an initial temperature of 300°K we find that $\varepsilon_0 = 7.79 \times 10^8$ ergs/g for argon and $\varepsilon_0 = 7.80 \times 10^9$ ergs/g for helium.

To check our results with thoe of Lutzky and Lehto,[16] the nondimensional maximum radius $\lambda_{max} = R_{2_{max}}/L_E$ was found for each explosion. From Fig. 4 we found that λ_{max} was constant for each combination of target and background gas. To find if our values of λ_{max} agreed with those of the numerical computations, we plotted λ_{max} as a function of $\varepsilon_1/\varepsilon_0$ and included points which could be calculated from the publications of previous investigators. This is shown in Fig. 6. Error bars indicate standard deviations. There was good correlation between experimental

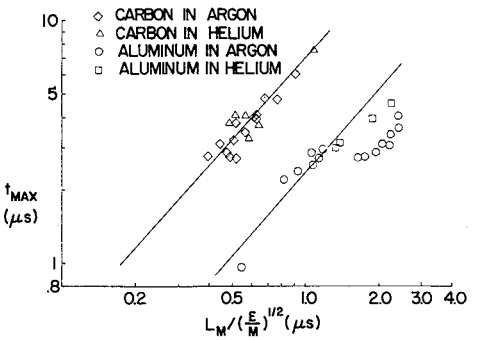

Fig. 9 Dependence of the time at which the secondary shock wave is at its maximum radius on the characteristic time $L_M/(E/M)^{1/2}$.

and numerical values. By inspection of Fig. 6, an empirical relation between λ_{max} and $\varepsilon_1/\varepsilon_0$ can be expressed as

$$\lambda_{max} = 0.8(\varepsilon_1/\varepsilon_0)^{-1/3} \tag{10}$$

It can be shown that Eq. (10), follows directly from the result shown by Fig. 5. From Fig. 5 we see that

$$R_{2_{max}} = 0.95 L_M \tag{11}$$

From the definitions of L_E and L_M

$$\frac{\varepsilon_1}{\varepsilon_0} = \frac{E/M}{\frac{3}{2}p_0/\rho_0} = \frac{2}{3}\left(\frac{L_E}{L_M}\right)^3 \tag{12}$$

From Eqs. (11) and (12) we find that

$$R_{2_{max}}/L_E = \lambda_{max} = 0.83(\varepsilon_1/\varepsilon_0)^{-1/3} \tag{13}$$

This result agrees very closely with Eq. (10).

Measurements were also made of t_{max} and t_{ret}. Again in agreement with Lutzky and Lehto,[16] for a given value of $\varepsilon_1/\varepsilon_0$, the nondimensionalized times given by $t_{max}(L_E/a_0)^{-1}$ and $t_{ret}(L_E/a_0)^{-1}$ were nearly constant. Figures 7 and 8 show plots of these times as functions of $\varepsilon_1/\varepsilon_0$ for the present data as well as previous numerical results. The numerical results show that these characteristic times for explosions of gas spheres which are at the same temperature as the ambient atmosphere appear to follow a relation

$$t_{ret}/(L_E/a_0) \sim t_{max}/(L_E/a_0) \sim (\varepsilon_1/\varepsilon_0)^{-1} \tag{14}$$

The data from the present experiment exhibit the $(\varepsilon_1/\varepsilon_0)^{-1}$ dependence, but each target material required a different constant of proportionality. The TNT explosion computed by Brode agrees closely with our carbon driven explosions.

In analogy with the primary shock wave equivalence principle proposed earlier, we nondimensionalize the times of maximum radius and return of the secondary shock with respect to $L_M/(E/M)^{1/2}$. Plots of t_{max} and t_{ret} as functions of this characteristic time are given in Figs. 9 and 10. Although t_{max}

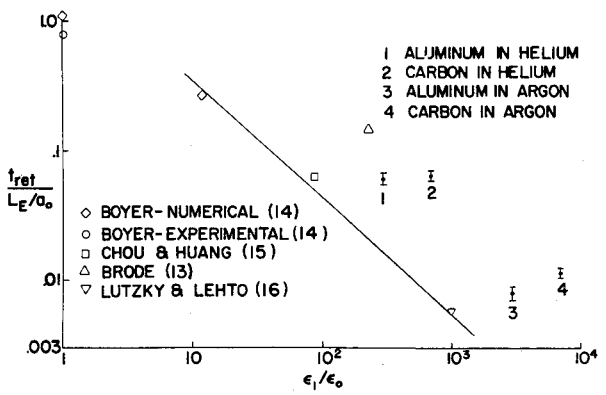

Fig. 8 Dependence of the nondimensional time at which the secondary shock wave returns to the origin on the initial specific energy ratio.

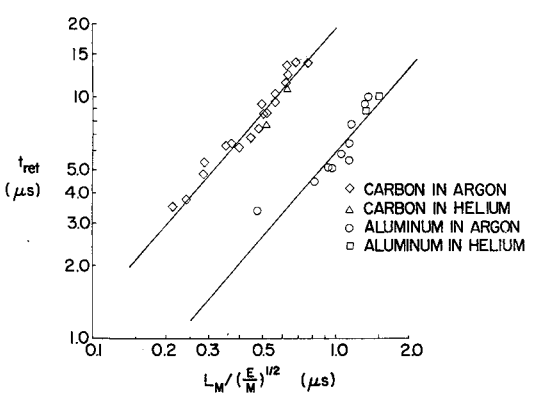

Fig. 10 Dependence of the time at which the secondary shock wave returns to the origin on the characteristic time $L_M/(E/M)^{1/2}$.

shows greater scatter than t_{ret}, a definite trend is evident. For each target material, t_{max} and t_{ret} depended only on the characteristic time, $L_M/(E/M)^{1/2}$. The scatter of the t_{max} measurements was due to the diffuse nature of the secondary shock wave in explosions with large L_M. Thus the behavior of the secondary shock wave exhibited an equivalence principle, in that for all explosions the maximum radius depended only on the characteristic time $L_M/(E/M)^{1/2}$ although the precise relationship for each target material was different.

Conclusions

Previous studies[7,9] of laser-produced explosions have shown no effect of the mass of the driver plasma on the motion of the primary shock wave. The data presented here show systematic effects of the driver mass. For $R < L_M$ the primary shock wave trajectories for various conditions were given by $0.5 < y < 0.7$ (with $R \sim t^y$). Only for $R > L_M$ did the exponent, y, approach the blast wave value of 2/5.

In addition, a secondary shock wave was observed and photographed. Comparisons were made with previous numerical solutions of spherical explosion problems to determine general rules of shock wave behavior. The results of the experiments indicated a small time equivalence for both the primary and secondary shock waves. The significant length scale was $L_M = (M/\rho_0)^{1/3}$; the significant time scale was $L_M/(E/M)^{1/2}$.

References

[1] Linlor, W. I., "Ion Energies Produced by Laser Giant Pulse," *Applied Physics Letters*, Vol. 3, 1963, p. 210.

[2] David, C., Arizonis, P. V., Weichel, H., Bruce, C., and Pyatt, K. D., "Density and Temperature of a Laser-Induced Plasma," *IEEE Journal of Quantum Electronics*, Vol. QE-2, 1966, p. 493.

[3] David, C. D., "Two Wavelength Interferometry of a Laser-Produced Carbon Plasma," *Applied Physics Letters*, Vol. 11, 1967, p. 394.

[4] Demtröder, W. and Jantz, W., "Investigation of Laser Produced Plasmas from Metal Surfaces," *Plasma Physics*, Vol. 12, 1970, p. 691.

[5] David, C. and Weichel, H., "Temperature of a Laser-Heated Carbon Plasma," *Journal of Applied Physics*, Vol. 40, 1969, p. 3674.

[6] Seka, W., Breton, C., Schwab, J. L., and Minier, C., "Temperature Measurements of a Laser-Produced Plasma Using the Recombination Continuum," *Plasma Physics*, Vol. 12, 1970, p. 73.

[7] Basov, N. G., Krokhin, O. N., and Sklizkov, G. V., "Formation of a Shock Wave with the Aid of Powerful Laser Radiation," *JETP Letters*, Vol. 6, 1967, p. 168.

[8] Bobin, J. L., Durand, Y. A., Langer, P. P., and Tonon, G., "Shock Wave Generation in Rarefied Gases by Laser Impact on Beryllium Targets," *Journal of Applied Physics*, Vol. 39, 1968, p. 4184.

[9] Hall, R. B., "Laser Production of Blast Waves in Low Pressure Gases," *Journal of Applied Physics*, Vol. 40, 1969, p. 1941.

[10] Taylor, G. I., "The Formation of a Blast Wave by a Very Intense Explosion," *Proceedings of the Royal Society*, Vol. 201A, 1950, p. 159.

[11] Sedov, L. I., *Similarity and Dimensional Methods in Mechanics*, Academic Press, New York, 1959, pp. 146–304.

[12] Robb, B. S., "Laser Produced Spherical Shock Waves," Ph.D. thesis, 1972, Dept. of Mechanical and Aerospace Engineering, Cornell Univ., Ithaca, N.Y.

[13] Brode, H. L., "Blast Wave from a Spherical Charge," *The Physics of Fluids*, Vol. 2, 1959, p. 217.

[14] Boyer, D. W., "An Experimental Study of the Explosion Generated by a Pressurized Sphere," *Journal of Fluid Mechanics*, Vol. 9, 1960, p. 401.

[15] Chou, P. C. and Huang, S. L., "Late Stage Equivalence in Spherical Blasts as Calculated by the Method of Characteristics," *Journal of Applied Physics*, Vol. 40, 1969, p. 752.

[16] Lutzky, M. and Lehto, D. L., "Scaling of Spherical Blasts," *Journal of Applied Physics*, Vol. 41, 1970, p. 844.

[17] Whitham, G. B., "On the Propagation of Shock Waves through Regions of Non-Uniform Area or Flow," *Journal of Fluid Mechanics*, Vol. 4, 1958, p. 337.

[18] Friedman, M. P., "A Simplified Analysis of Spherical and Cylindrical Blast Waves," *Journal of Fluid Mechanics*, Vol. 11, 1961, p. 1.